JOURNAL OF CATALYSIS **98**, 7–16 (1986)

Influence of Support Composition on the Reduction of Nitric Oxide over Rhodium Catalysts

NUTAN K. PANDE AND ALEXIS T. BELL

Department of Chemical Engineering, University of California, Berkeley, California 94720

Received April 4, 1985; revised September 17, 1985

The NO reduction by CO and H_2 over Rh/SiO_2, Rh/Al_2O_3, Rh/MgO, Rh/La_2O_3, and Rh/TiO_2 was investigated. Support composition was found to influence the activity, but not the selectivity of Rh. Exceptionally high low-temperature activity was obtained with Rh/TiO_2. The rate parameters for NO reduction over Rh/TiO_2 are distinctly different from those for all other catalysts. The high activity of Rh/TiO_2 is attributed to the presence of catalytically active centers on the support as well as on the surface of the supported Rh crystallites.

INTRODUCTION

The current catalysts used for the control of automotive emissions contain rhodium to promote the reduction of nitric oxide. Platinum and palladium are also present and serve to catalyze the oxidation of CO and hydrocarbons. The high cost of rhodium combined with the fact that it must be utilized in a ratio with platinum and palladium much higher than that found in nature provides a strong incentive to reduce or eliminate the content of rhodium in automotive converters. The results of several recent studies suggest that this might be accomplished by altering the support composition. For example, Rives-Arnau and Munuera (*1*) have shown that Rh/TiO_2 is more active than Rh/SiO_2 for NO reduction by CO, and Nakamura *et al.* (*2, 3*) have shown that Rh, Pt, and Pd supported on TiO_2 are more active for NO reduction by CO than catalysts prepared using SiO_2 or Al_2O_3 as the support. The effects of support composition have also been observed for nonnoble metal catalysts. Iizuka *et al.* (*4*) have examined the influence of support composition on NO reduction by H_2 over Fe_2O_3. They reported that Fe_2O_3 supported on SiO_2 was the most active catalyst, and Fe_2O_3 supported on SnO_2 the least active. In a study of NO reduction by H_2 and NH_3, Hattori *et al.* (*5*) reported that MoO_3/ZrO_2 was the most active catalyst for NO reduction by H_2 and MoO_3/TiO_2 was the most active catalyst for NO reduction by NH_3.

The present investigation was undertaken to determine the influence of support composition on NO reduction over Rh. Both H_2 and CO were used as reducing agents. Light-off characteristics and reaction kinetics were determined using a recycle reactor. Additional information was obtained from temperature-programmed desorption experiments.

EXPERIMENTAL

Catalyst Preparation

The supported catalysts were prepared using $RhCl_3 \cdot 3H_2O$ (Aldrich Chemicals) as the metal precursor. The composition, source, and BET surface area of each support are listed in Table 1. Samples of approximately 4 wt% Rh were prepared by incipient wetness impregnation of the support with a solution of $RhCl_3$ dissolved in deionized water. Following introduction of $RhCl_3$, each sample was dried overnight in a vacuum oven at 338 K and calcined in a 21% O_2/He mixture at 773 K for 1 h. The Rh weight loading of each sample was determined by X-ray fluorescence. The Rh dispersion was measured by volumetric che-

0021-9517/86 $3.00

TABLE 1

Support and Catalyst Properties

Catalyst	Source of support	Support surface area (m^2/g)	Rh loading (%)	D_{Rh}
Rh/SiO_2	Cab-O-Sil HS-5	250	4.60	0.55
Rh/Al_2O_3	Degussa	175	4.16	0.64
Rh/MgO	Mallinckrodt	100	4.58	0.46
Rh/TiO_2	Degussa P-25	50	4.33	0.26
Rh/La_2O_3	Ventron	14	4.23	0.10

misorption of H_2 at room temperature on samples which were reduced overnight at 573 K. The Rh/La_2O_3 was characterized based on nitric oxide uptake. This was necessary due to a large spillover of H_2 to the support (6). A summary of the catalyst and support properties is given in Table 1.

Catalyst Evaluation

The experimental apparatus and techniques used in this study have been described previously (7, 8). Reaction rates were measured using a small reactor with external recycle. Fresh reactants were continuously supplied to the recycle loop and products were withdrawn for analysis by gas chromatography (9). The recycle ratio for the reactor was 200 to 1.

Each catalyst charge was determined so as to provide 1.82×10^{19} Rh surface atoms. Preceding each run, the catalyst was reduced in 100% H_2 at 573 K for at least 24 h. The reduction period was ended by purging the reactor loop with helium. Prior to collecting rate data, the reaction of NO with CO or NO with H_2 was allowed to proceed for 15–20 h. The catalyst activity and selectivity at the end of this period were stable.

Temperature-Programmed Desorption of NO

The interaction of NO with each catalyst was studied by temperature-programmed desorption. The apparatus used for these measurements has been described previously (10). A 30-mg sample of the catalyst was placed in a quartz microreactor and reduced in H_2 for 18 h at 573 K. The catalyst was then evacuated, and the temperature ramped in vacuum to 823 K. For the Rh/La_2O_3 catalyst, the evacuation temperature was limited to 573 K, to avoid complete suppression of chemisorption due to migration of support material onto the metal as a result of high-temperature exposure (6). The sample was subsequently cooled under vacuum to room temperature. The microreactor was repressurized with helium, and NO was pulsed to the reactor to achieve saturation coverage of the catalyst. The catalyst was then ramped to 823 K at a linear heating rate of 1 K/s in a helium stream flowing at 50 cm^3/min.

An investigation was made as well of the interaction of NO with each catalyst following its use for NO reduction by H_2. For these studies, the catalyst was either prereduced or preoxidized. In the former case, the sample was reduced in H_2 for 18 h at 573 K. The sample was then cooled to room temperature, and the reaction feed mixture of 1% NO/2% H_2 in He was introduced to the microreactor at 200 cm^3/min. The sample was then slowly heated to a temperature at which point the conversion of NO was 15%. The sample was maintained under reaction conditions at this temperature for 2 h. The catalyst was then evacuated at the reactor temperature and cooled in vacuum to room temperature. The microreactor was repressurized with helium, and NO was pulsed to the reactor to achieve saturation coverage of the catalyst. The catalyst was then ramped to 823 K at a linear heat-

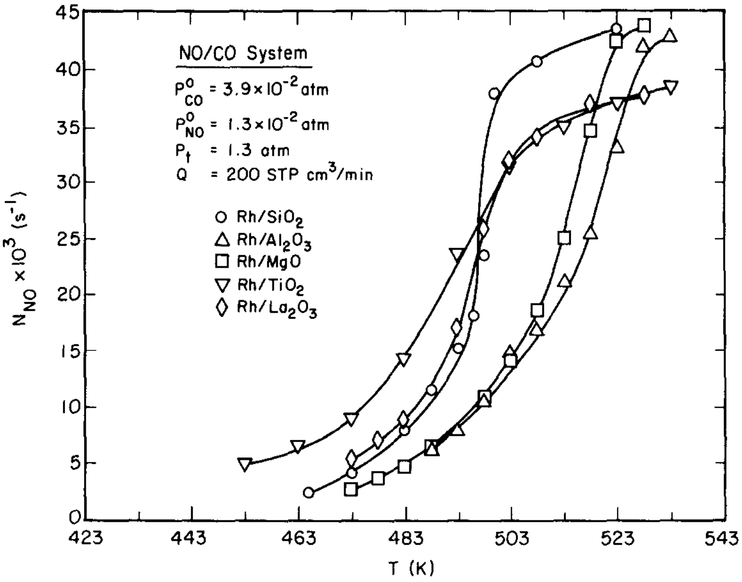

FIG. 1. Effect of temperature on activity for NO reduction by CO.

ing rate of 1 K/s in a helium stream flowing at 50 cm³/min.

The interaction of NO with preoxidized catalysts was studied using a similar procedure. In this case, the catalyst was first reduced in H_2 for 18 h at 573 K and then oxidized in a 1% NO/He mixture flowing at 200 cm³/min for 2 h. The remainder of the procedure was followed as described above.

RESULTS

Reduction of NO by CO

Figure 1 shows the activity for NO reduction by CO as a function of temperature for each catalyst. The results for Rh/SiO_2 are those reported by Hecker and Bell (7). The activity for the reduction of NO by CO depends on support composition, and for conversions below ~50% decreases in the following order: $Rh/TiO_2 > Rh/La_2O_3 \approx Rh/SiO_2 > Rh/MgO \approx Rh/Al_2O_3$. For conversions above 50%, Rh/TiO_2 and Rh/La_2O_3 exhibit comparable activities and both are less active than Rh/SiO_2. The influence of temperature on the selectivities to N_2O and N_2 are shown in Fig. 2 for Rh/TiO_2. The selectivity to N_2O increases from 65% at 453 K to a maximum of 80% at 503 K, then decreases to 70% at 533 K. Similar patterns were observed for the other catalysts. A comparison of product selectivities at fixed reaction rates is presented in Table 2.

The kinetics of NO reduction by CO

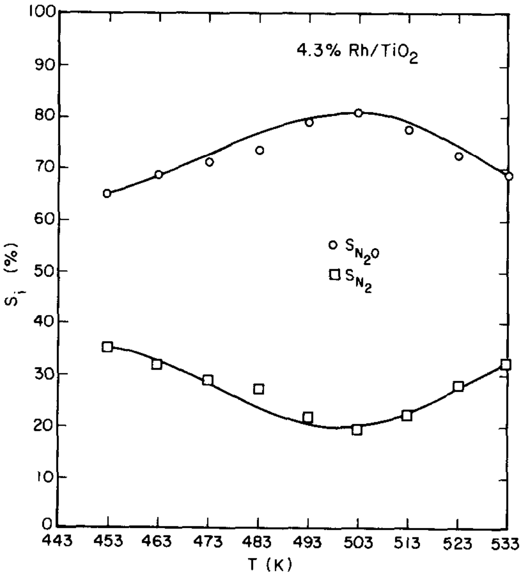

FIG. 2. Effect of temperature on product distribution for Rh/TiO_2 during NO reduction by CO ($P^\circ_{CO} = 3.9 \times 10^{-2}$ atm, $P^\circ_{NO} = 1.3 \times 10^{-2}$ atm, $P_t = 1.3$ atm, Q = 200 (STP) cm³/min).

TABLE 2

Influence of Support Composition on Product Selectivity for NO Reduction by CO

	$N_{NO} = 15 \times 10^{-3}\ s^{-1}$		$N_{NO} = 40 \times 10^{-3}\ s^{-1}$	
Catalyst	S_{N_2O}	S_{N_2}	S_{N_2O}	S_{N_2}
Rh/SiO_2	80	20	70	30
Rh/Al_2O_3	77	23	75	25
Rh/MgO	80	20	75	25
Rh/TiO_2	72	28	67	33
Rh/La_2O_3	85	15	65	35

TABLE 3

Kinetic Parameters for NO Reduction by CO

Catalyst	E_a (kcal/mol)	α	β	k_{NO} (at 483 K)
Rh/SiO_2	33.5	−0.17	+0.08	4.3×10^{-3}
Rh/Al_2O_3	24.2	−0.37	+0.03	0.82×10^{-3}
Rh/MgO	25.8	−0.15	+0.06	2.92×10^{-3}
Rh/TiO_2	19.6	+0.09	−0.22	7.75×10^{-3}
Rh/La_2O_3	30.2	−0.16	+0.04	4.75×10^{-3}

Note. $N_{NO} = k_{NO}P_{NO}^{\alpha}P_{CO}^{\beta}$; $k_{NO} = \text{atm}^{-(\alpha+\beta)}\ s^{-1}$.

were investigated for NO conversions below 30%. The dependences on NO and CO partial pressures were determined at 483 K, and the apparent activation energy was determined at NO and CO partial pressures of 1.3×10^{-2} and 3.9×10^{-2} atm, respectively. A summary of the rate parameters for each of the catalysts is given in Table 3. Rh/SiO_2, Rh/Al_2O_3, Rh/MgO, and Rh/La_2O_3 are characterized by a negative dependence on NO partial pressure and a weakly positive dependence on CO partial pressure. The partial pressure dependences for Rh/TiO_2 are notably different—the NO dependence is weakly positive and the CO dependence is negative. The apparent activation energy for NO reduction by CO decreases in the order $Rh/SiO_2 > Rh/La_2O_3 > Rh/MgO > Rh/Al_2O_3 > Rh/TiO_2$.

Reduction of NO by H_2

Figure 3 shows the turnover frequency for NO reduction by H_2 as a function of temperature for each of the catalysts. Here again, the results for Rh/SiO_2 are those reported by Hecker and Bell (*11*). It is immediately apparent that the activity of Rh/TiO_2 is substantially greater than that of the remaining catalysts, and that the order of decreasing activity is $Rh/TiO_2 \gg Rh/Al_2O_3 \gtrsim Rh/La_2O_3 > Rh/SiO_2 \gtrsim Rh/MgO$. The product selectivity for Rh/TiO_2 is shown in Fig. 4. For temperatures between 373 and 433 K, the N_2O selectivity increases gradually

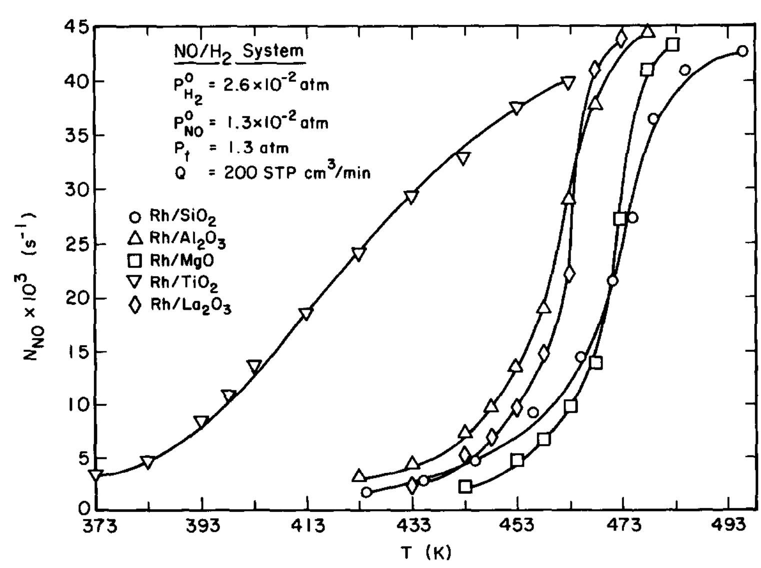

FIG 3. Effect of temperature on activity for NO reduction by H_2.

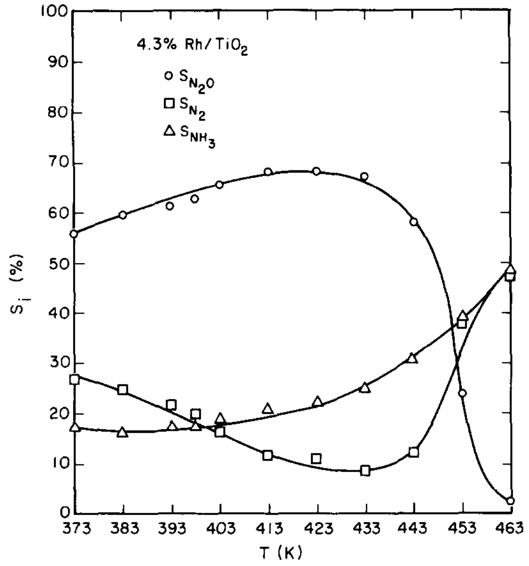

FIG. 4. Effect of temperature on product distribution for Rh/TiO_2 during NO reduction by H_2 ($P^{\circ}_{H_2} = 2.6 \times 10^{-2}$ atm, $P^{\circ}_{NO} = 1.3 \times 10^{-2}$ atm, $P_t = 1.3$ atm, $Q = 200$ (STP) cm^3/min).

from 55 to 65%, the NH_3 selectivity increases from 17 to 25%, and the N_2 selectivity decreases from 28 to 10%. As the temperature is raised above 433 K, the selectivity to N_2O rapidly decreases to zero while the selectivities to N_2 and NH_3 increase to ~50%. Similar product distributions were observed with each of the other catalysts. A comparison of the product selectivities at fixed reaction rates is presented in Table 4.

The kinetics of NO reduction by H_2 were also investigated for NO conversions below 30%. The dependences on NO and H_2 partial pressures were determined at 443 K, and the apparent activation energy was determined at NO and H_2 partial pressures of 1.3×10^{-2} and 2.6×10^{-2} atm, respectively. The rate parameters obtained for each catalyst are summarized in Table 5. The rate of NO reduction over Rh/SiO_2, Rh/Al_2O_3, Rh/MgO, and Rh/La_2O_3 is characterized by a negative dependence on NO and a positive dependence on H_2. The kinetics for NO reduction over Rh/TiO_2 stand out in that the dependences on NO and H_2 partial pressures are both positive. The apparent activation energy for NO reduction by H_2 decreases in the order Rh/MgO > Rh/La_2O_3 > Rh/Al_2O_3, Rh/SiO_2 > Rh/TiO_2.

TABLE 4

Influence of Support Composition on Product Selectivity for NO Reduction by H_2

Catalyst	$N_{NO} = 15 \times 10^{-3}$ s^{-1}			$N_{NO} = 40 \times 10^{-3}$ s^{-1}		
	S_{N_2O}	S_{N_2}	S_{NH_3}	S_{N_2O}	S_{N_2}	S_{NH_3}
Rh/SiO_2	62	17	21	10	40	50
Rh/Al_2O_3	70	20	10	10	52	38
Rh/MgO	65	28	7	18	58	24
Rh/TiO_2	66	13	21	2	49	49
Rh/La_2O_3	76	8	16	8	55	37

TABLE 5

Kinetic Parameters for NO Reduction by H_2

Catalyst	E_a (kcal/mol)	α	β	k_{NO}
Rh/SiO_2	21.9	−0.22	+0.59	20.10×10^{-3} (443 K)
Rh/Al_2O_3	23.1	−0.40	+0.62	11.20×10^{-3} (443 K)
Rh/MgO	27.5	−0.32	+0.60	4.47×10^{-3} (443 K)
Rh/TiO_2	16.3	+0.51	+0.51	0.31 (383 K)
Rh/La_2O_3	25.5	−0.26	+0.71	20.90×10^{-3} (443 K)

Note. $N_{NO} = k_{NO}P^{\alpha}_{NO}P^{\beta}_{H_2}$; k_{NO} = atm$^{-(\alpha+\beta)}$ s^{-1}.

Temperature-Programmed Desorption Spectroscopy

Temperature-programmed desorption spectroscopy was used to assess the effects of support composition on the nature of the interactions of NO with Rh. Figures 5–9 illustrate the TPD spectra obtained following NO adsorption on freshly reduced catalyst samples. The temperature of maximum

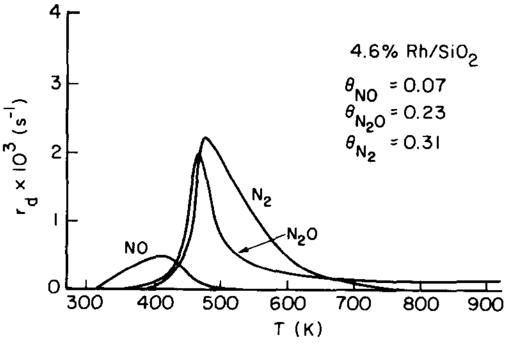

FIG. 5. NO TPD spectrum for reduced 4.6% Rh/SiO_2.

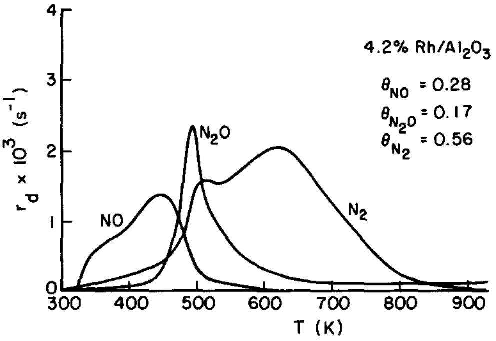

FIG. 6. NO TPD spectrum for reduced 4.2% Rh/Al$_2$O$_3$.

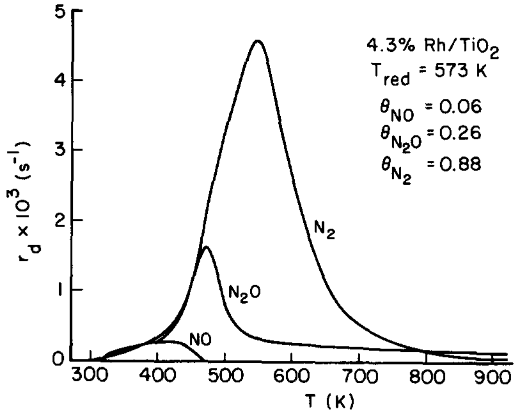

FIG. 8. NO TPD spectrum for reduced 4.3% Rh/TiO$_2$.

release of each product is listed in Table 6, and the extent of NO conversion to N_2 and N_2O (D_{NO}), the distribution of nitrogen-containing products, and the uptake of NO are listed for each catalyst in Table 7.

The TPD spectra in Figs. 5–9 are qualitatively similar. Desorption of molecular NO is the first process to occur as the temperature increases. This is followed by NO decomposition to form N_2O and then N_2. N_2 formation occurs over a broader temperature range than N_2O formation and is not completed until 773 K. The extent of NO decomposition, represented by D_{NO} in Table 7, decreases in the order $La_2O_3 > TiO_2 > SiO_2 \gtrsim Al_2O_3 \approx MgO$. A very similar trend is also seen for the fraction of N_2 formed. Table 6 shows as well that the temperature at which the release of each nitrogen-containing product reaches a maximum depends on the suport composition. The following sequences are observed: T_{NO}, $La_2O_3 < TiO_2 \approx SiO_2 < Al_2O_3 \approx MgO$; T_{N_2O}, $La_2O_3 < TiO_2 \approx SiO_2 < Al_2O_3 \approx MgO$; T_{N_2}, $La_2O_3 < SiO_2 < MgO < TiO_2 < Al_2O_3$.

To determine whether exposure of the catalysts to reaction conditions altered their characteristics for NO desorption and decomposition, TPD spectra were taken following the reduction of NO with H_2 over Rh/SiO$_2$, Rh/Al$_2$O$_3$, Rh/TiO$_2$, and Rh/La$_2$O$_3$. The spectra for these catalysts are presented in Figs. 10-13 and characteristic features determined from these spectra are given in Table 8.

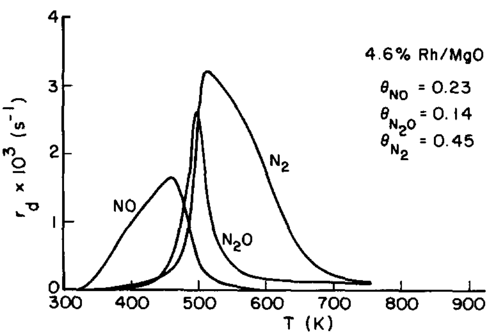

FIG. 7 NO TPD spectrum for reduced 4.6% Rh/MgO.

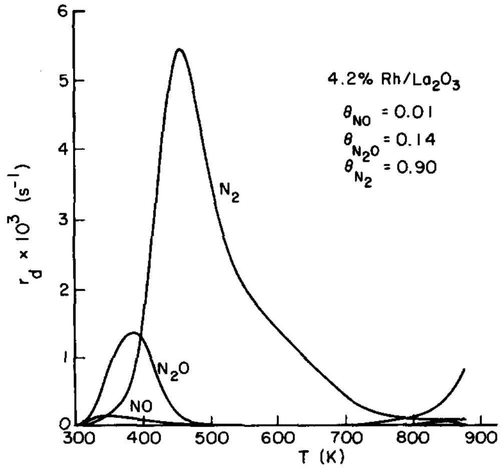

FIG. 9. NO TPD spectrum for reduced 4.2% Rh/La$_2$O$_3$.

TABLE 6

Peak Desorption Temperatures

Catalyst	T_{NO} (K)	T_{N_2O} (K)	T_{N_2} (K)
Rh/SiO_2	423	473	483
Rh/Al_2O_3	443	493	503,623
Rh/MgO	453	493	508
Rh/TiO_2	423	473	548
Rh/La_2O_3	373	<373	454

With limited exceptions, the spectra in Figs. 10–13 are similar to those in Figs. 5, 6, 8, and 9. The primary differences are evident from a comparison of the N_2O spectra. In the spectra taken after exposure to reaction conditions, the N_2O peak is narrower than that observed in the spectra taken with freshly reduced catalyst. For Rh/SiO_2, in addition to the narrow N_2O peak at 473 K, there is also a broad N_2O peak at 750 K. This feature is not present in the TPD spectrum of a Rh/SiO_2 sample oxidized in NO prior to being exposed to reaction conditions, nor in the spectrum taken with a freshly reduced Rh/SiO_2 sample (see Fig. 5).

The trends in extent of NO conversion to N_2 and N_2O and fraction of N_2 formation seen in Table 7 are similar to those seen in Table 8. The value of D_{NO} decreases in the order $La_2O_3 > TiO_2 \gtrsim Al_2O_3 > SiO_2$. Since the temperatures at which NO, N_2O, and N_2 reach a maximum rate of release, seen in Figs. 10–13, are virtually the same for all four catalysts, it is not possible to order T_{NO}, T_{N_2O}, or T_{N_2} according to support composition.

Comparison of the results in Tables 7 and 8 reveals that while the distribution of products formed over the freshly reduced catalyst samples and those first subjected to reaction conditions are, for the most part, similar, there are notable differences in the

TABLE 7

No TPD Product Distribution (%) and Extent of NO Conversion to N_2 and N_2O for Reduced Catalysts

Catalyst	θ°_{NO}[a]	X_{NO} (%)	X_{N_2O} (%)	X_{N_2} (%)	D_{NO}[b] (%)
Rh/SiO_2	0.61	11	38	51	70
Rh/Al_2O_3	1.01	28	17	56	65
Rh/MgO	0.82	28	17	55	65
Rh/TiO_2	1.20	5	22	73	84
Rh/La_2O_3	1.05	1	13	86	93

[a] Expressed in equivalents of a Rh monolayer.

[b] $D_{NO} = (\frac{1}{2}X_{N_2O} + X_{N_2})$.

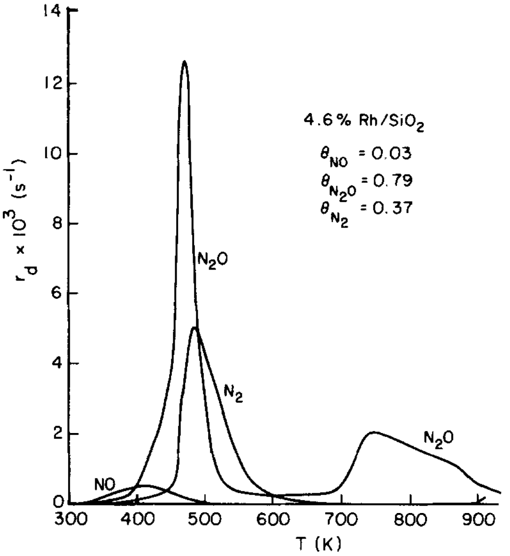

FIG. 10. NO TPD spectrum for 4.6% Rh/SiO_2 after NO/H_2 reduction.

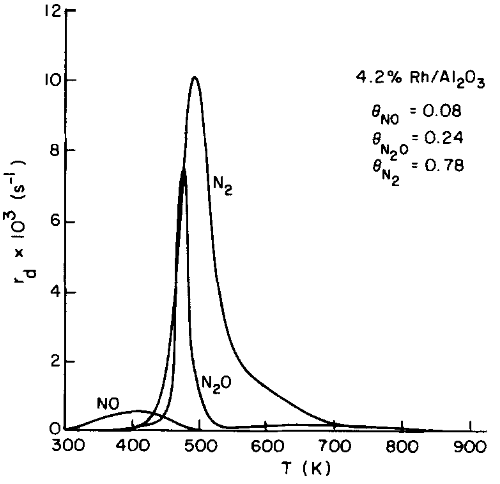

FIG. 11. NO TPD spectrum for 4.2% Rh/Al_2O_3 after NO/H_2 reduction.

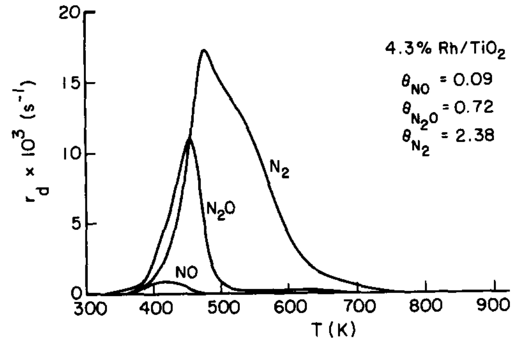

FIG. 12. NO TPD spectrum for 4.3% Rh/TiO_2 after NO/H_2 reduction.

total amount of NO adsorbed on Rh/SiO_2 and Rh/TiO_2 between the two cases. For Rh/SiO_2, the NO uptake increases from 0.61 of a Rh monolayer on the freshly reduced sample to 1.19 of a Rh monolayer on a reduced sample exposed to reaction conditions. Most of this increase though is due to the appearance of the high-temperature N_2O peak. A similarly large increase is not observed for a Rh/SiO_2 sample preoxidized prior to exposure to reaction conditions. For Rh/TiO_2, the total NO uptake increases from 1.2 Rh monolayers up to 3.25 Rh monolayers.

DISCUSSION

The influence of support composition on the specific rate of NO reduction by either CO or H_2 is clearly demonstrated by the present results. The observation that Rh/TiO_2 is more active than Rh/SiO_2 or Rh/Al_2O_3 for NO reduction by CO is in good qualitative agreement with the results reported by Rives-Arnau and Munuera (*1*) and by Nakamura et al., (*2, 3*). Since the kinetics of NO reduction were not measured by these authors, comparisons of rate parameters are not possible.

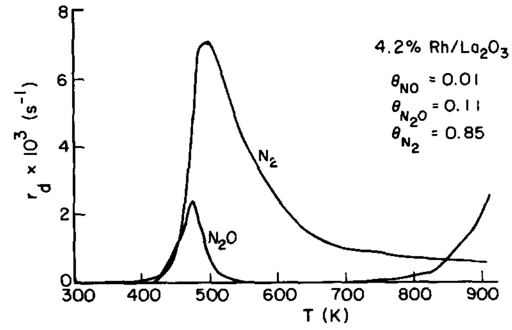

FIG. 13. NO TPD spectrum for 4.2% Rh/La_2O_3 after NO/H_2 reduction.

TABLE 8

NO TPD Product Distribution (%) and Extent of NO Conversion to N_2 and N_2O for Catalysts after NO/H_2 Reduction

Catalyst	θ^0_{NO}[a]	X_{NO} (%)	X_{N_2O} (%)	X_{N_2} (%)	D_{NO}[b] (%)
Rh/SiO_2	1.19	2.6	66.6[c]	30.8	64
Rh/Al_2O_3	1.10	6.9	22.3	70.8	82
Rh/TiO_2	3.25	2.6	22.1	73.3	84
Rh/La_2O_3	0.97	0.5	11.6	88.1	94

[a] Expressed in equivalents of a Rh monolayer.

[b] $D_{NO} = (\frac{1}{2}X_{N_2O} + X_{N_2})$.

[c] Includes both N_2O peaks.

Hecker and Bell (*7, 11*) have shown that the kinetics of NO reduction by CO and H_2 over Rh/SiO_2 can be interpreted on the basis of a mechanism in which the dissociation of NO is the rate-limiting step to NO reduction. For reduction by CO, this process was presumed to occur via direct dissociation at a vacant Rh site, whereas for reduction by H_2, atomic hydrogen was postulated to assist in the dissociation process. The similarity of the power-law dependences on NO and CO or H_2 partial pressures for Rh/Al_2O_3, Rh/MgO, and Rh/La_2O_3 to those for Rh/SiO_2 suggest that the mechanism and nature of the rate-limiting step on all of these catalysts are similar. The markedly different values of the dependences for Rh/TiO_2, together with the substantially lower activation energy, suggest that either the mechanism of NO reduction is different on Rh/TiO_2, or, alternatively, that the same mechanism prevails for all catalysts but that the rate-limiting step is different. We believe that the second of these possibilities is more likely since it is observed that the distribution of products obtained by NO reduction with either H_2 or

CO is more or less the same regardless of support composition.

Previous studies of N_2 and N_2O formation during NO desorption from Rh (*12*) or during NO reduction over Rh (*7, 11*) have shown that the dissociation of adsorbed NO is a necessary first step. In view of this, it is reasonable to ask whether the exceptionally high activity of Rh/TiO_2 might not be due to its effectiveness in dissociating NO. One measure of the effectiveness of a catalyst in NO dissociation is the extent to which NO is converted to N_2 and N_2O during NO TPD, D_{NO}. Tables 7 and 8 demonstrate that while the value of D_{NO} for Rh/TiO_2, 84%, is higher than that for Rh/SiO_2, Rh/Al_2O_3, and Rh/MgO, all of which are less active NO reduction catalysts, it is lower than that for Rh/La_2O_3, 93%, a catalyst which is also less active than Rh/TiO_2. Thus, the magnitude of D_{NO} does not provide a satisfactory basis for identifying and interpreting the high reduction activity of Rh/TiO_2. A similar conclusion can also be drawn about the temperature for the onset of N_2 and N_2O formation during TPD. For example, Figs. 5–9 show that significant rates of N_2O and N_2 formation are observed above 300 K for Rh/Al_2O_3, Rh/TiO_2, and Rh/La_2O_3, and Figs. 10–12 show significant rates of N_2O and N_2 formation above 350 K for Rh/SiO_2 and Rh/TiO_2.

Table 8, however, does reveal a characteristic of Rh/TiO_2 which distinguishes it from all the other catalysts; this is the large value of θ_{NO}° measured when NO is adsorbed on the catalyst immediately following its use for NO reduction by H_2. Thus, $\theta_{NO}^{\circ} = 3.25$ for Rh/TiO_2, but θ_{NO}° is closer to 1.0 for all of the other catalysts. It is interesting to note in this connection that a similarly high value of θ_{NO}° (2.28) for Rh/TiO_2 has been measured following NO reduction with CO (*13*). Values of θ_{NO}° exceeding unity suggest that on used Rh/TiO_2, NO can adsorb both on the surface of Rh particles and on the surface of the support. Pande and Bell (*14*) have recently reported that NO will adsorb on TiO_2 as well as Rh, and that the interaction of NO with TiO_2 is strongly affected by its state of reduction. Of particular interest is the observation that partially reduced TiO_2 will effect the decomposition of NO to form N_2 and N_2O. In contrast, reduced La_2O_3 does not dissociate molecular NO (*6*). Thus, it appears that the high activity of Rh/TiO_2 for NO reduction by CO or H_2 may be due to catalysis occurring on the support as well as on the supported metal particles. Activation of the TiO_2 is presumed to occur by the spillover of atomic hydrogen from Rh particles onto the support and subsequent reduction of the support surface. Further evidence for the participation of the support in NO reduction over Rh/TiO_2 will be presented separately (*14*).

CONCLUSIONS

Support composition strongly influences the catalytic activity, but not the selectivity, of Rh for NO reduction by CO and H_2. Exceptionally high low-temperature activity is achieved using TiO_2 as the support. The rate parameters are also distinctly different for Rh/TiO_2 compared to the remaining catalysts, Rh/SiO_2, Rh/Al_2O_3, Rh/MgO, and Rh/La_2O_3. The high activity of Rh/TiO_2 is attributed to the presence of catalytically active centers on the support as well as on the surface of the supported Rh crystallites. It is proposed that activation of the support occurs by partial reduction of the support.

ACKNOWLEDGMENT

This work was supported by the National Science Foundation through Grant CPE82-16537.

REFERENCES

1. Rives-Arnau, V., and Munuera, G., *Appl. Surf. Sci.* **6,** 122 (1980).
2. Nakamura, R., Nakai, S., Sugiyama, K., Echigoya, E., *Bull. Chem. Soc. Jpn.* 54, 1950 (1981).
3. Nakamura, R., Yamagami, K., Nishiyama, S., Niiyama, H., and Echigoya, E., *Chem. Lett.* No. 2, 275 (1981).

4. Iizuka, T., Ikeda, H., Terao, T., and Tanabe, K., *Aust. J. Chem.* **35,** 927 (1982).
5. Hattori, H., Tanabe, K., Tanaka, K., and Okazaki, S., *in* Proceedings, 3rd Int. Conf. Chem. and Uses of Molybdenum" (1979).
6. Pande, N. K., and Bell, A. T., unpublished results.
7. Hecker, W. C., and Bell, A. T., *J. Catal.* **84,** 200 (1983).
8. Hecker, W. C., Ph.D. thesis. University of California, Berkeley, 1982.
9. Hecker, W. C., and Bell, A. T., *Anal. Chem.* **53,** 817 (1981).
10. Low, G., and Bell, A. T., *J. Catal.* **57,** 397 (1979).
11. Hecker, W. C., and Bell, A. T., *J. Catal.* **92,** 247 (1985).
12. Chin, A. A., and Bell, A. T., *J. Phys. Chem.* **87,** 3700 (1983).
13. Pande, N. K., and Bell, A. T., *Appl. Catal.,* in press.
14. Pande, N. K., and Bell, A. T., *J. Catal.,* in press.